R-matrix analyses for the ^{7}Li(t, n) ^{9}Be and ^{7}Li$(^3$He, $p)$ ^{9}Be reactions and their improved thermonuclear reaction rates

J. Hu [1,3,*] N. Tian [1,2,3] Y. Y. Li,[1,3] S. Q. Hou [1,3] S. W. Xu,[1,3] J. B. Liu,[1,3] and J. F. Lv[2]

[1]*Institute of Modern Physics, Chinese Academy of Sciences, Lanzhou 730000, China*
[2]*School of Nuclear Science and Technology, Lanzhou University, Lanzhou 730000, China*
[3]*School of Nuclear Science and Technology, University of Chinese Academy of Sciences, Beijing 100049, China*

R-matrix analyses have been performed for the ^{7}Li(t, n) ^{9}Be and ^{7}Li$(^3$He, $p)$ ^{9}Be reactions, which are thought to be of importance in primordial abundance of ^{9}Be. All available data were compiled and used in the R-matrix analysis. The resonance parameters are compared with previous works. The resulting fit was used to extract an improved determination of the reaction rate for both reactions. The present rates of ^{7}Li(t, n_0) ^{9}Be at $T = 0.3$–3 GK are about 7.5–28.9% lower than the values of Brune *et al.* and are larger than the rates of Barhoumi *et al.* by up to 28.1%. Our ^{7}Li$(^3$He, $p_0)$ ^{9}Be rates are higher than those of Yan *et al.* by no more than 29% and differ within 21% from those of Rath *et al.* over 0.1–3.0 GK.

I. INTRODUCTION

Primordial nucleosynthesis of ^{9}Be is thought to provide a definitive test for cosmological models of the big bang [1,2]. These rare and fragile nuclei are not generated in the normal course of stellar nucleosynthesis and are, in fact, destroyed in hydrogen burning in stellar interiors, especially via (p, α) reactions. The standard model (SM) is well known to reproduce the primordial abundances of several light nuclides (^{2}H, ^{3}He, and ^{4}He) [3,4]. In this model, the density of the universe at the time of primordial nucleosynthesis is assumed to be uniform. However, some of the predicted primordial abundances are very sensitive to the assumption of uniform density. In studies using the nonuniform density model (NDM), density fluctuations are allowed and the universe is assumed to be separated into two regions at the onset of nucleosynthesis: a high-density proton-rich region and a low-density neutron-rich region. The abundances of ^{3}H, ^{3}He, and ^{7}Li are both quite high in the neutron-rich region. Thus the ^{7}Li(t, n) ^{9}Be and ^{7}Li$(^3$He, $p)$ ^{9}Be reactions could process the ^{7}Li to ^{9}Be and contribute significantly to synthesis of ^{9}Be in that region.

The light elements' abundances observed in metal-poor halo stars are expected to reflect primordial nucleosynthesis [5]. Boyd and Kajino [1,2] claimed that the observed ^{9}Be abundance in these stars could be of the same order as that predicted from NDM by including the ^{7}Li(t, n) ^{9}Be and ^{7}Li$(^3$He, $p)$ ^{9}Be reactions. However, it has been clarified that the ^{9}Be abundance is well understood to arise from cosmic-ray spallation processes and cannot be interpreted as evidence of a big-bang nucleosynthesis (BBN) contribution to ^{9}Be. Better reaction rates for ^{9}Be-producing reactions are important for constraining nonstandard cosmological models. To improve the precision of these reaction rates, the experimental cross section or S factor is desirable.

The low-energy reaction cross section of ^{7}Li(t, n) ^{9}Be has been measured by Barhoumi *et al.* [6] and Brune *et al.* [7]. The two different sets of the measured cross section agree well with each other in the low-energy region $E_{c.m.} < 600$ keV. However, they deviate from each other at higher energies and their difference amounts to a discrepancy by a factor of 2 at $E_{c.m.} \approx 900$ keV. An alternative way to estimate the cross section for the ^{7}Li(t, n) ^{9}Be reaction is to use the cross section of ^{7}Li$(^3$He, $p)$ ^{9}Be. Rath *et al.* [8] measured the low-energy cross sections of ^{7}Li$(^3$He, $p)$ ^{9}Be and converted the ^{7}Li$(^3$He, $p)$ ^{9}Be cross sections to those for ^{7}Li(t, n) ^{9}Be. While their estimated reaction rates agreed circumstantially with the assumptions of Boyd and Kajino [1], nearly an order of magnitude difference was found compared to the experimental reaction rates from Barhoumi *et al.* [6] and Brune *et al.* [7].

The first ^{7}Li$(^3$He, $p)$ ^{9}Be measurement for astrophysical application was performed by Rath *et al.* [8], who determined the astrophysical S factor of ^{7}Li$(^3$He, $p)$ ^{9}Be in the energy range from $E_{c.m.} = 0.5$ to 2.0 MeV. Later, Yan *et al.* [9] performed a new measurement of the ^{7}Li$(^3$He, $p)$ ^{9}Be cross section at energies below the center of the Gamow peak. Their results are approximately 40% lower than the extrapolations of Rath *et al.* [8] and Yamamoto *et al.* [10], indicating a significantly lower direct-process contribution. The calculated reaction rates are lower than the values of Rath *et al.* in the temperature range $T_9 = 0.1$–0.9.

In the present paper we perform the first R-matrix analysis for both reactions. The details of the analysis are described in Sec. II. The revised reaction rates are presented in Sec. III. Finally, this work is summarized in Sec. IV. It is worth noting that the reaction rates of ^{7}Li(t, n) ^{9}Be and ^{7}Li$(^3$He, $p)$ ^{9}Be determined in this work are those to the ^{9}Be ground state

*hujunbaggio@impcas.ac.cn

only, since all excited states of ^{9}Be decay in some manner into $2\alpha + n$, which cannot lead to ^{9}Be synthesis.

II. *R*-MATRIX ANALYSIS

In the previous analyses of the astrophysical *S* factors of ^{7}Li$(t, n)^9$Be and ^{7}Li$(^3$He$, p)^9$Be reactions [6–9], a simple sum of Breit-Wigner functions representing different resonances was fitted to obtain the resonance energy and total width. In this case, the direct reaction component was assumed to be constant for simplification. In addition, any interference effects between levels as well as nonresonant background were neglected. To make a more precise estimation for the reaction rates, a rigorous and comprehensive analysis of *S* factors is required.

The *R*-matrix formalism is a crucial tool in the study of nuclear astrophysics reactions. The introduction of *R*-matrix theory allows for more reliable interpretation of the observed experimental data, since it makes it possible to accurately account for interference effects between multiple resonant and nonresonant contributions.

A multichannel, multilevel *R*-matrix code AZURE2 [11] was used for the analysis. Initial values for resonance energies, widths, and spin parities are taken from Ref. [12]. These values are often provide a good starting point for the *R*-matrix fit. Cross sections, *S* factors, and particle partial widths throughout this work are always in the center-of-mass system. The current comprehensive analysis allows for several additional constraints on the *R*-matrix fit which have not been fully considered in past analyses. More available data from other reaction channels are considered to provide additional constraints. Since the γ branches are expected to be weak, the γ channels are neglected in the analysis. The *R*-matrix calculations are also done in the Brune parametrization [13], allowing for the direct use of observable level energies and widths.

For the following *R*-matrix fitting plots, center-of-mass energy is given on the bottom horizontal axis and the excitation energy on the top horizontal axis of the plot.

A. ^{7}Li$(t, n)^9$Be

^{10}Be is the compound nucleus of the ^{7}Li$(t, n)^9$Be reaction. The present analysis considers one particle entrance channel, ^{7}Li $+ t$, and two particle exit channels, ^{9}Be $+ n$ and ^{6}He $+ \alpha$ (see Fig. 1). Three energy levels near the ^{7}Li $+ t$ separation threshold are taken into account in the analysis.

Only two measurements of the ^{7}Li$(t, n)^9$Be cross section at Gamow energy have been reported, by Barhoumi *et al.* [6] and Brune *et al.* [7], respectively. Although these two are in reasonable agreement with each other, it appears that the cross section is affected by the nearest threshold resonance, for which resonance parameters were not determined in either experiment.

Later, Yamamoto *et al.* [10] investigated the reaction mechanism of ^{7}Li$(t, n)^9$Be through comparison with both experimental data [6,7]. To estimate the resonance parameters of the nearest threshold state, they made two assumptions using knowledge of the ^{7}Li$(^3$He$, p)^9$Be reaction. Finally, they
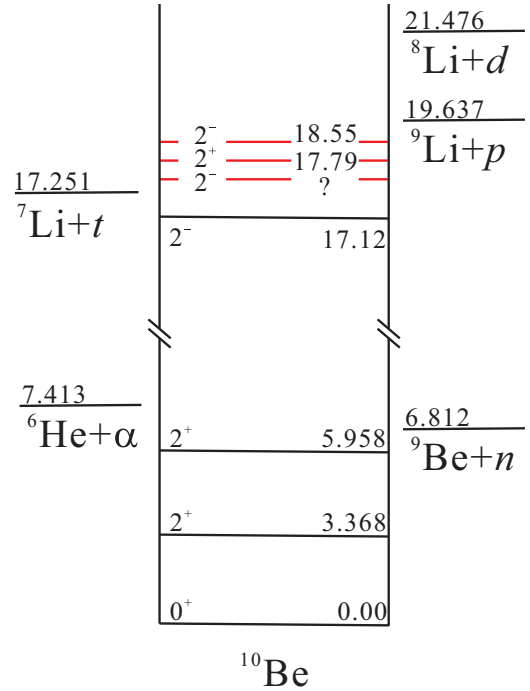

FIG. 1. Level scheme of the ^{10}Be compound nucleus.

constrained theoretically the upper and lower limits of the total cross section of ^{7}Li$(t, n)^9$Be.

In the present *R*-matrix analysis, experimental data from the Refs. [6,7] are considered simultaneously (see Fig. 2). Both data sets are obtained from the EXFOR database [14]. The error bars of the data by Barhoumi *et al.* [6] are unavailable, thus we digitized the errors from Fig. 6 in Ref. [6].
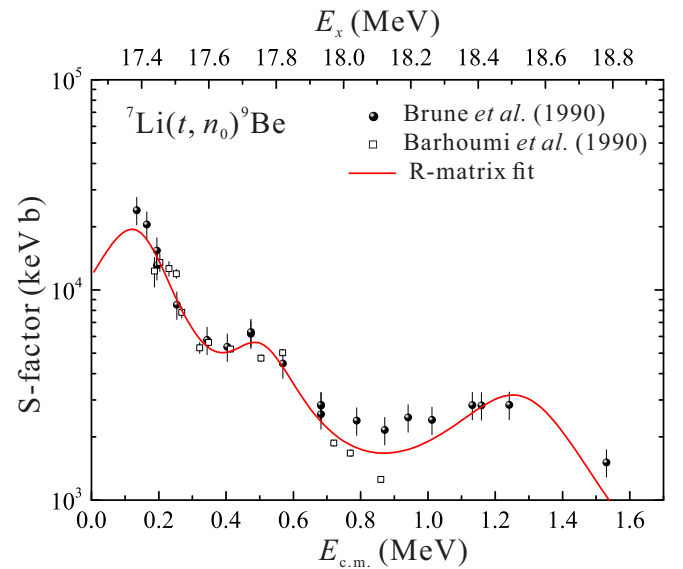

FIG. 2. *R*-matrix fit to the total ^{7}Li$(t, n_0)^9$Be cross-section data of Barhoumi *et al.* [6] and Brune *et al.* [7]. The last datum of Brune *et al.* [7] around $E_{\text{c.m.}} = 1.5$ MeV is derived from the inverse reaction ^{9}Be$(n, ^3$H$_{0+1})$ [15] and ^{9}Be$(n, ^3$H$_1)$ [16] measurements via the principle of detailed balance.

TABLE I. The relevant energy levels of ^{10}Be from the present *R*-matrix fit, compared with previous works. Γ_n^* is the total neutron width for decay to the first through ninth excited states in ^{9}Be.

	Present work						Barhoumi *et al.* [6]		Brune *et al.* [7]	
No.	E_x (MeV)	J^π	Γ_t (keV)	Γ_{n0} (keV)	Γ_n^* (keV)	Γ_α (keV)	Γ_{tot} (keV)	E_x (MeV)	Γ_{tot} (keV)	E_x (MeV)	Γ_{tot} (keV)
1.	17.380	2^-	1.83	5.44	270		277.27	17.251–17.401	140	17.279	170
2.	17.753	2^+	2.83	223	1.12	11.44	238.39	17.802	150	17.744	211
3.	18.550	2^-	77.7	285.56	69.7		432.96			18.540	862

The relevant particle separation energies are shown in Fig. 1. The channel radii $a_t = 4.967$ fm, $a_n = 4.312$ fm, and $a_\alpha = 4.766$ fm are used for the triton channel, neutron channel, and α-particle channel, respectively. The experimental results of Brune *et al.* [7] clearly showed that the decays to excited states in ^{9}Be dominated the cross section. Thus, we considered all the possible neutron decay channels, from the first to ninth excited states, and allowed them to be free parameters during the fit. The best overall *R*-matrix fitting curve is shown in Fig. 2 and the resonant parameters obtained are listed in Table I.

The first level, which is theoretically expected to lie very close to the ^{7}Li + t threshold, has not been observed in any experiments. Our fitted $E_x = 17.380$ MeV is about 100 keV larger than the value of Brune *el al.*. Γ_{tot}, which is dominated by the neutron channels, is more than 100 keV larger than the results of Brune *et al.* and Barhoumi *et al.*. Lacking data at $E_{c.m.} \leqslant 200$ keV, Barhoumi *et al.* performed the fits for resonance energy E_r in the range 0–150 keV with a step size of 50 keV. The total width was fixed as 140 keV during these fits. They claimed that the reaction rates were merely impacted on a minor level with the variation of E_r.

For the second level, the fitted $E_x = 17.753$ MeV and $\Gamma_{tot} = 238.39$ keV are in good agreement with the results of Brune *et al.* [7]. Since this state has natural parity, the α reaction channel is open. However, no ^{6}He + α data were reported at the relevant energies; we therefore allow the Γ_α to vary as a free parameter throughout the fitting.

We fixed the E_x of the third level as $E_x = 18.55$ MeV, otherwise a reasonable fit cannot be obtained. Barhoumi *et al.* did not consider this state due to the lack of data at $E_{c.m.} > 900$ keV. Our fitted Γ_{tot} is smaller than the value reported by Brune *et al.*. The reason is that our *R*-matrix curve was dragged to the data of Barhoumi *et al.* around $E_{c.m.} = 700$–900 keV. Another independent and high precision measurement of the cross section is expected to solve this discrepancy between these two experiments.

The astrophysical *S* factor is dominated by the two resonant contributions at the low energies $E_{c.m.} \leqslant 1.0$ MeV. The Gamow window energy of the ^{7}Li(t, n)^{9}Be reaction is 250 keV, corresponding to 0.8 GK, which is a typical temperature in primordial nucleosynthesis. At this energy region the *S* factor is strongly subject to the unmeasured resonance parameters of the nearest threshold state. Compared to the previous results, there is a large deviation for the resonance parameters of the first level based on our *R*-matrix analysis. Thus, more data points of the cross section below $E_{c.m.} = 150$ keV are needed to improve the prospective *R*-matrix analysis.

B. ^{7}Li(^{3}He, p) ^{9}Be

Rath *et al.* performed the first ^{7}Li(^{3}He, p)^{9}Be measurement for astrophysical application [8]. A simple Breit-Wigner fit was performed using two known resonances ($E_r = 0.66$ and 0.98 MeV) and a constant direct reaction component. Later, Yamamoto *et al.* [10] examined the reaction mechanism of ^{7}Li(^{3}He, p)^{9}Be. A theoretical curve, which is the incoherent sum of direct reaction and compound resonance ($E_r = 0.643$, 1.01, and 1.51 MeV) contributions, was calculated to describe the observed data of Rath *et al.*. The most recent experimental determination of ^{7}Li(^{3}He, p)^{9}Be dates back to 2002, where Yan *et al.* [9] measured the cross sections at effective center-of-mass energies of $E_{c.m.} = 106.3$ and 112.8 keV. Yan *et al.* incorporated their data with all other published information [8,17–19] to derive an *S*-factor description.

It is known that ^{10}B, which is the compound nucleus of the ^{7}Li + ^{3}He nuclear system, has three resonance states at energies near the ^{7}Li + ^{3}He separation threshold (see Fig. 3). Unlike the case of ^{7}Li(t, n)^{9}Be, more reaction channels are open in the analysis of ^{7}Li(^{3}He, p)^{9}Be. The inclusion of other channel data in the fitting procedure provides strong

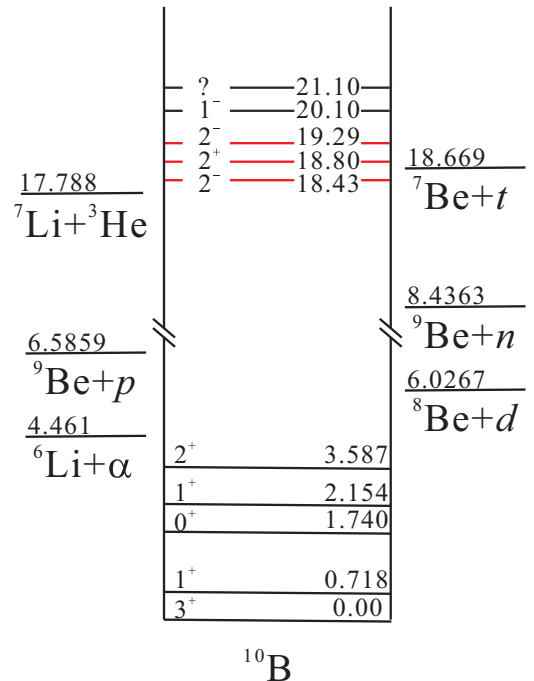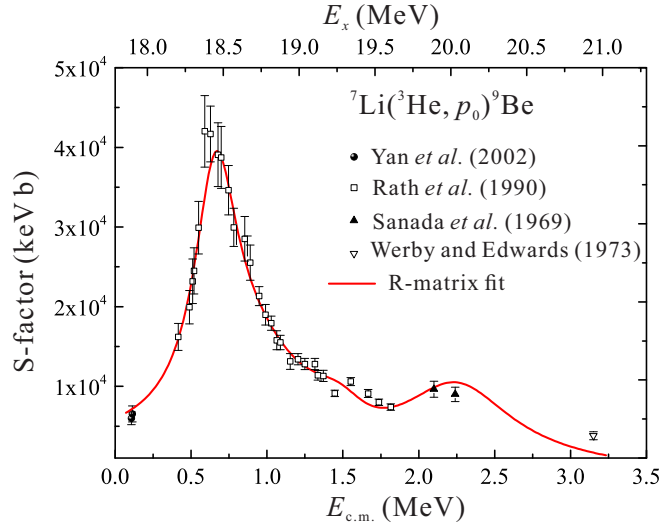FIG. 3. Level scheme of the ^{10}B compound nucleus.

FIG. 4. *R*-matrix fit to the total $^7\text{Li}(^3\text{He}, p_0)^9\text{Be}$ cross-section data of previous works [8,9,17,18].

FIG. 5. *R*-matrix fit to the $^7\text{Li}(^3\text{He}, p_1)^9\text{Be}$ differential cross sections of Lru *et al.* at $\theta_{\text{lab}} = 120°$ [20].

constraints on the *R*-matrix fits since the resonance energies and particle widths are identical. We therefore consider more data from these additional reaction channels.

The following subsections detail the different particle reaction channels included in this analysis. Although they are described individually, the fits to the different particle-reaction-channel data sets were performed simultaneously.

A channel radius of $a_{^3\text{He}} = 4.697$ fm is used for the entrance channel $^7\text{Li} + ^3\text{He}$. For the exit channels, $a_{np} = 4.312$ fm is used for neutron and all proton channels, $a_\alpha = 4.766$ fm for all α channels, and $a_d = 4.564$ fm for the deuteron channel. We did not consider the triton channel in the analysis because the triton separation energy is very close to the energy levels investigated here. Γ_t is tiny compared to other exit reaction channels and can be neglected in the analysis. The simultaneous *R*-matrix fit for multiple channels is much more complicated than the single-channel fit, and the energy levels considered here are known very well. Therefore, we fixed the excitation energies for all the levels, otherwise it would be very difficult to obtain a reasonable fit.

I. $^7\text{Li}(^3\text{He}, p)^9\text{Be}$: Included in the analysis are the *S* factors of ground-state transition p_0 from Table I of Ref. [9], the differential cross sections of first-excited-state transition p_1 from Ref. [20] (retrieved from EXFOR [14]), and the total cross sections of second-excited-state transition p_2 from Fig. 4 of Ref. [8] (retrieved from EXFOR [14]). The *R*-matrix fitting curves for $^7\text{Li}(^3\text{He}, p_{0,1,2})^9\text{Be}$ are shown in Figs. 4–6 respectively.

II. $^7\text{Li}(^3\text{He}, n)^9\text{B}$: Excitation functions of $^7\text{Li}(^3\text{He}, n_0)^9\text{B}$ were studied at $\theta_{\text{lab}} = 0°$, $90°$, and $160°$ by Din and Weil [21]. Two prominent resonances at $E_x = 19.3$ and 20.1 MeV are seen at $\theta_{\text{lab}} = 0°$. At $90°$ and $160°$, the yield curves are relatively featureless. Therefore, we only adopted the data set at $\theta_{\text{lab}} = 0°$ to perform the fit. The data sets were extracted from the EXFOR database [14]. The error bars are unavailable; a 1% uncertainty was set arbitrarily to all data
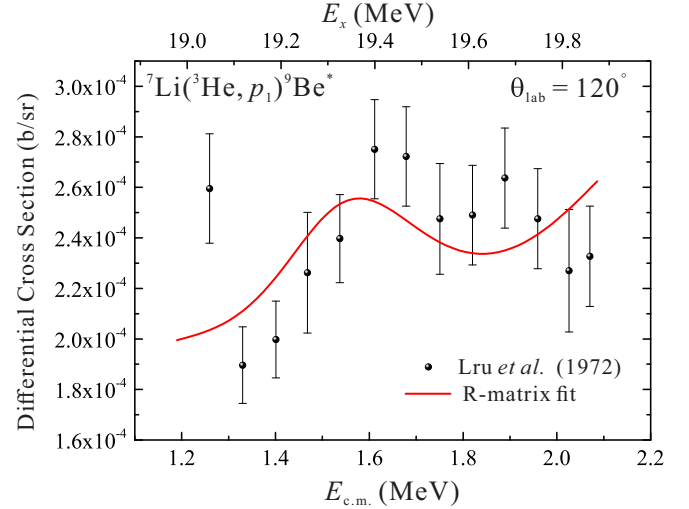
points. No information from the excited-state transition could be obtained, thus we simply assume the Γ_n is dominated by Γ_{n_0}. The *R*-matrix fitting curve for $^7\text{Li}(^3\text{He}, n_0)^9\text{B}$ is shown in Fig. 7.

III. $^7\text{Li}(^3\text{He}, \alpha)^6\text{Li}$: The differential cross sections for the $^7\text{Li}(^3\text{He}, \alpha)^6\text{Li}$ leading to the ground, first excited, and second excited states of ^6Li were measured by Forsyth and Perry [22]. The excitation curves for the α_0 group are striking in that they vary considerably between the three angles studied. A clear resonance at $E_x = 19.3$ MeV was observed at $\theta_{\text{lab}} = 8°$. It was attempted to expand the analysis to higher energies, but because the data have less structure in this region, reasonable fits could not be obtained. During the fitting, the high energy data are removed. The α_1 group also shows
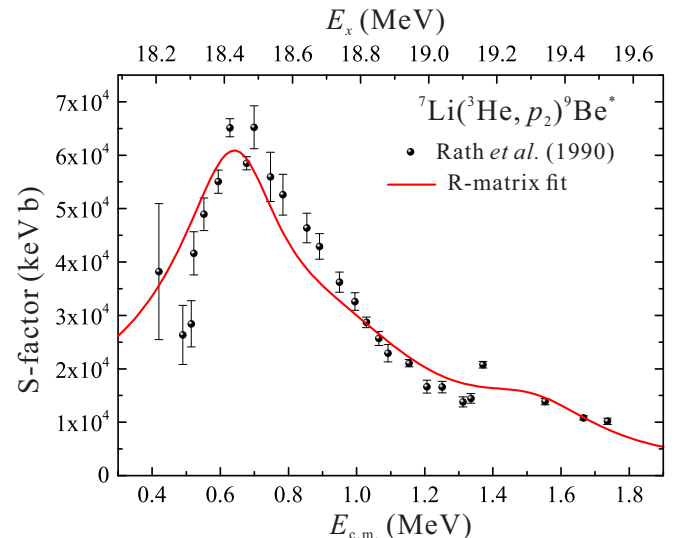

FIG. 6. *R*-matrix fit to the total $^7\text{Li}(^3\text{He}, p_2)^9\text{Be}$ cross-section data of Rath *et al.* [8].

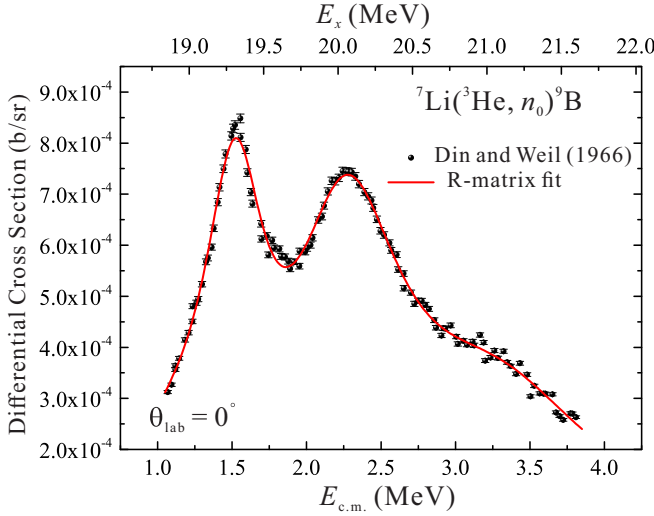FIG. 7. *R*-matrix fit to the ^{7}Li(^{3}He, n_0)^{9}B differential sections of Din and Weil at $\theta_{\text{lab}} = 0°$ [21].

FIG. 9. *R*-matrix fit to the ^{7}Li(^{3}He, α_2)^{6}Li differential cross sections of Forsyth and Perry at $\theta_{\text{lab}} = 90°$ [22].

a resonance at $E_x = 19.57$ MeV in its 8° yield. However, no other works reported this resonance. The α_1 data are questionable, so we did not include it in the fit and allowed the α_1 width to vary as a free parameter. The α_2 group corresponding to the ^{7}Li(^{3}He, α_2)^{6}Li reaction leading to the 3.56 MeV state of ^{6}Li was measured at 90°. Two peak structures at $E_x = 18.8$ and 20.1 MeV were observed in the excitation curve. All the data points of α channels are obtained from the EXFOR database [14]. The *R*-matrix fitting curves for ^{7}Li(^{3}He, $\alpha_{0,2}$)^{9}Be are shown in Figs. 8 and 9 respectively.

It was attempted to include the data from the deuteron reaction channel [23,24]; however, no reasonable fit can be achieved using either experimental data set. Thus we have to allow the Γ_d to vary as a free parameter in the fit, indicating that improved cross section data of the ^{7}Li(^{3}He, d)^{9}B reaction are needed.
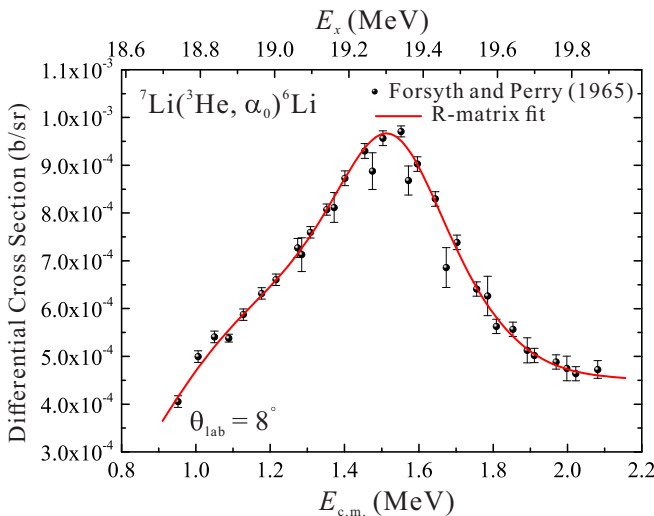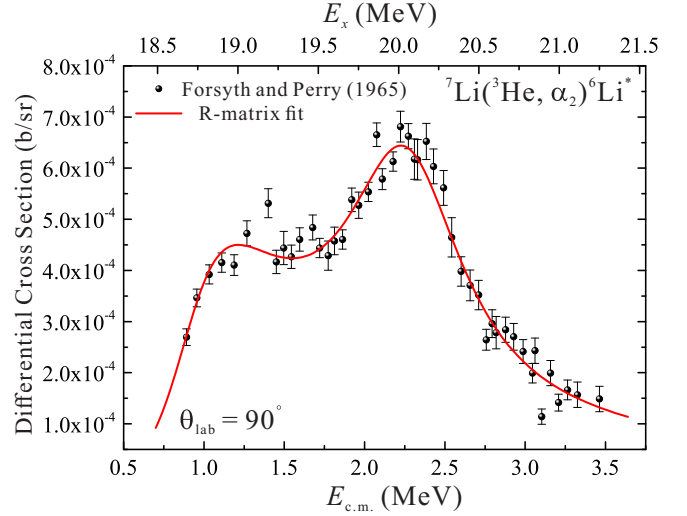
Five energy levels were included in our *R*-matrix analysis and the fitted resonance parameters are listed in Table II. For ^{7}Li(^{3}He, p_0)^{9}Be, all the data points were from the Table I of Yan *et al.*. We did not include the last data point at $E_{\text{c.m.}} = 6.99$ MeV, as it is too far away from the other ones. Rath *et al.* [8] only included the first two levels in the analysis to reproduce their data. Yan *et al.* [9] involved two more states in the analysis, as they introduced more published data points at higher energies. The Γ_{tot} of the first level, $E_x = 18.43$ MeV, is in excellent agreement with previous results. However, there is a large discrepancy for the Γ_{tot} of the second level at $E_x = 18.80$ MeV. The same situation happened at the third level, whose Γ_{tot} is more than twice larger than that of Yan *et al.*. In contrast, our fourth level's Γ_{tot} is comparable with the result of Yan *et al.*. The fifth level at $E_x = 21.1$ MeV works like a background level, whose resonance parameters are not at all determined. Without this level, our fits deviate from the data points considerably.

III. ASTROPHYSICAL REACTION RATE

The thermonuclear reaction rates for both reactions were calculated by numerical integration of the following equation [25]:

$$N_A \langle \sigma v \rangle = \left(\frac{8}{\mu \pi} \right)^{\frac{1}{2}} \frac{N_A}{(kT)^{\frac{3}{2}}}$$
$$\times \int_0^\infty S(E) \exp \left(-\frac{E}{kT} - bE^{-1/2} \right) dE, \quad (1)$$

where N_A is Avogadro's number, μ is the reduced mass in the entrance channel, k is the Boltzmann constant, T is the temperature, and E is the energy in the center of mass. Only the reaction channel of the ground state transition leads to ^{9}Be synthesis, thus, the improved reaction rates for the reactions

FIG. 8. *R*-matrix fit to the ^{7}Li(^{3}He, α_0)^{6}Li differential cross sections of Forsyth and Perry at $\theta_{\text{lab}} = 8°$ [22].

TABLE II. The relevant energy levels of ^{10}B from the present R-matrix fit, compared with previous works. The sign of the partial widths indicates the sign of the interference. E_x is in units of MeV, particle widths are in units of keV.

No.	E_x	J^π	$\Gamma_{^3\text{He}}$	Γ_{p_0}	Γ_{p_1}	Γ_{p_2}	Γ_n	Γ_{α_0}	Γ_{α_1}	Γ_{α_2}	Γ_d	Γ_{tot}	Rath *et al.* [8]		Yan *et al.* [9]	
													E_x	Γ_{tot}	E_x	Γ_{tot}
1.	18.43	2^-	−10.22	10.08	−7.95	8.05	4.91	−2.13	−123.3		184.75	351.39	18.448	340	18.431	340
2.	18.80	2^+	104.04	15.78	12.31	48.63	−3.08	55.11	−40.29	−103.74	543.14	926.12	18.768	720	18.798	600
3.	19.34	2^-	65.4	18.31	3.77	−26.07	50.31	−49.7	−69.64		198.3	481.5			19.398	210
4.	20.10	1^-	485.24	171.80	1.61	−19.01	20.41	138.91	−0.12	72.15	0.38	909.63			20.098	1000
5.	21.10	1^-	−74.47	624.70	−220.16	−160.77	−393.11	49.67	−93.91	−6.43	6.9	1630.12				

^{7}Li(t, n_0)^{9}Be and ^{7}Li$(^3$He$, p_0)$^{9}Be were determined based on the resulting R-matrix fit.

A. ^{7}Li(t, n_0)^{9}Be rate

Figure 10 shows the ^{7}Li(t, n_0)^{9}Be rates from the previous and present works. Our rates are comparable with those presented by Barhoumi *et al.* [6] and Brune *et al.* [7]. In the temperature region of 0.3–3.0 GK, the present rates of ^{7}Li(t, n_0)^{9}Be are about 7.5–28.9% lower than the values of Brune *et al.* and are larger than those of Barhoumi *et al.* by up to 28.1%. The theoretical estimations made by Boyd and Kajino [1] and Malaney and Fowler [26] are in general higher than our rates. The rates of Rath *et al.* [8] inferred from the ^{7}Li$(^3$He$, p_0)$^{9}Be data are higher than ours by a factor of 4 to 7. This may indicate that the method of estimating reaction rates from similar reaction data could result in a large uncertainty. To improve the precision of the reaction rates, a future experiment should focus on the determination of the E_r of the nearest threshold level.

B. ^{7}Li$(^3$He$, p_0)$^{9}Be rate

Only two studies [8,9] reported the reaction rates of ^{7}Li$(^3$He$, p_0)$^{9}Be, as this reaction is less significant than ^{7}Li(t, n_0)^{9}Be. Figure 11 shows the comparison of the present ^{7}Li$(^3$He$, p_0)$^{9}Be rate with the previous rates. It can be seen

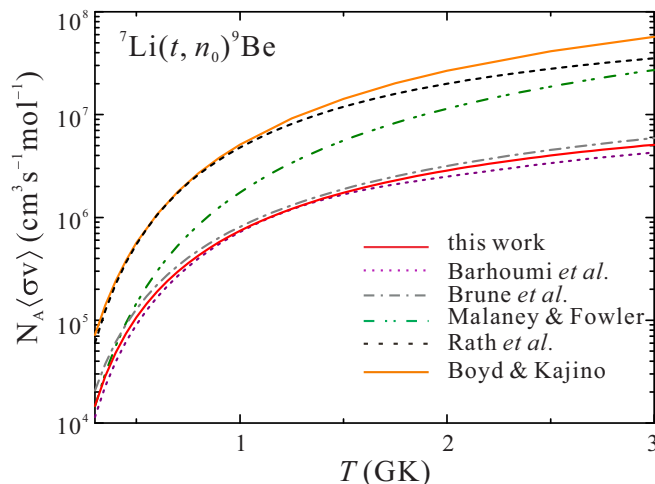that our rates are almost the same as previous ones at $T >$ 0.75 GK. The deviation becomes larger as the temperature decreases. In the temperature region of 0.1–3.0 GK, the present rates are higher than those of Yan *et al.* by 29% at most and differ within 21% from those of Rath *et al.*.

C. Other reaction rates

Based on the fitted resonance parameters, several dominant reaction rates, which should be included in the BBN calculation of ^{9}Be, are determined. Figure 12 shows all the reaction rates relevant to the primordial ^{9}Be abundance. Since the AZURE2 code cannot treat multiparticle breakup, we were not able to provide the reaction rates of ^{7}Li$(t, 2n)2$^{4}He and ^{7}Li$(^3$He$, np)2$^{4}He. These two reaction rates are adopted from Malaney and Fowler [26] based on the theoretical estimation.

IV. CONCLUSION

We performed the first R-matrix analyses for the ^{7}Li(t, n)^{9}Be and ^{7}Li$(^3$He$, p)$^{9}Be reactions, which are thought to be of importance in primordial nucleosynthesis of ^{9}Be. These rigorous fits with more physical meanings were able to satisfactorily reproduce the available cross-section data. Based on the fitted resonance parameters, revised reaction rates were calculated. In the temperature region of
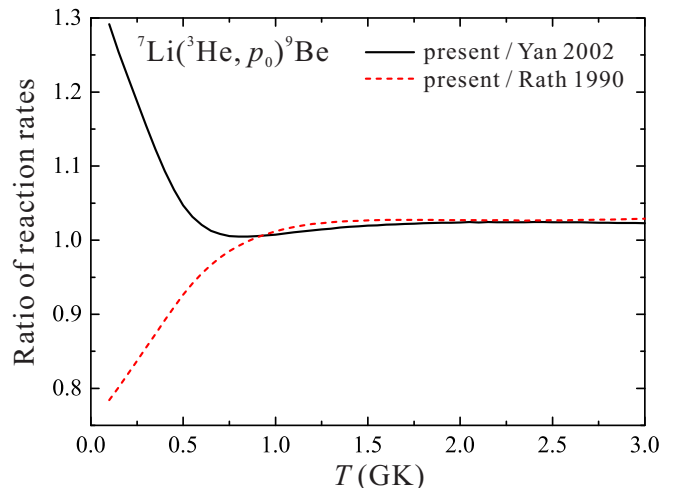

FIG. 10. Thermonuclear reaction rates for ^{7}Li(t, n_0)^{9}Be.

FIG. 11. A comparison of the present ^{7}Li$(^3$He$, p_0)$^{9}Be rate with the previous rates of Yan *et al.* [9] and Rath *et al.* [8].

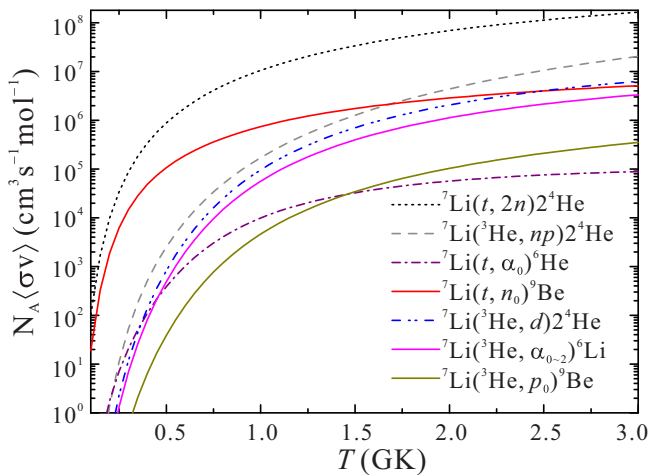FIG. 12. Thermonuclear reaction rates relevant to the primordial ^{9}Be abundance.

0.3–3.0 GK, our rates of ^{7}Li$(t, n_0)\,^9$Be are about 7.5–28.9% lower than the values of Brune *et al.* and are larger than the rates of Barhoumi *et al.* by up to 28.1%. For the ^{7}Li$(^3$He$, p_0)\,^9$Be reaction, even though some of the resonance parameters are quite different from earlier works, the revised reaction rates are consistent with their results at $T > 0.75$ GK. Our ^{7}Li$(^3$He$, p_0)\,^9$Be rates are higher than those of Yan *et al.* by no more than 29% and differ within 21% from those of Rath *et al.* over 0.1–3.0 GK. Compared to previous rates, our new rates of ^{7}Li$(t, n_0)\,^9$Be and ^{7}Li$(^3$He$, p_0)\,^9$Be do not change very much. It is understandable that differences in models, e.g., resonance parameters and interference effects, will not significantly change the reaction rate as long as the models describe the same data.

[1] R. Boyd and T. Kajino, Astrophys. J. **336**, L55 (1989).

[2] T. Kajino and R. Boyd, Astrophys. J. **359**, 267 (1990).

[3] A. M. Boesgaard and G. Steigman, Annu. Rev. Astron. Astrophys. **23**, 319 (1985).

[4] K. A. Olive, D. N. Schramm, G. Steigman, and T. P. Walker, Phys. Lett. B **236**, 454 (1990).

[5] L. M. Hobbs and C. Pilachowski, Astrophys. J. **334**, 734 (1988).

[6] S. Barhoumi, G. Bogaert, A. Coc, P. Aguer, J. Kiener, A. Lefebvre, J.-P. Thibaud, F. Baumann, H. Freiesleben, C. Rolfs, and P. Delbourgo-Salvador, Nucl. Phys. A **535**, 107 (1991).

[7] C. R. Brune, R. W. Kavanagh, S. E. Kellogg, and T. R. Wang, Phys. Rev. C **43**, 875 (1991).

[8] D. Rath, R. Boyd, H. Hausman, M. Islam, and G. Kolnicki, Nucl. Phys. A **515**, 338 (1990).

[9] J. Yan, F. E. Cecil, U. Greife, C. C. Jewett, R. J. Peterson, and R. A. Ristenin, Phys. Rev. C **65**, 048801 (2002).

[10] Y. Yamamoto, T. Kajino, and K.-I. Kubo, Phys. Rev. C **47**, 846 (1993).

[11] R. E. Azuma, E. Uberseder, E. C. Simpson, C. R. Brune, H. Costantini, R. J. de Boer, J. Görres, M. Heil, P. J. LeBlanc, C. Ugalde, and M. Wiescher, Phys. Rev. C **81**, 045805 (2010).

[12] D. Tilley, J. Kelley, J. Godwin, D. Millener, J. Purcell, C. Sheu, and H. Weller, Nucl. Phys. A **745**, 155 (2004).

[13] C. R. Brune, Phys. Rev. C **66**, 044611 (2002).

[14] V. Zerkin, 2011, http://www-nds.iaea.org/exfor/exfor.htm.

[15] H. Liskien, R. Widera, R. Wölfle, and S. M. Qaim, Nucl. Sci. Eng. **98**, 266 (1988).

[16] F. S. Dietrich, L. F. Hansen, and R. P. Koopman, Nucl. Sci. Eng. **61**, 267 (1976).

[17] J. Sanada, Y. C. Liu, Y. Sugiyama, and O. Mikoshiba, J. Phys. Soc. Jpn. **26**, 853 (1969).

[18] M. F. Werby and S. Edwards, Nucl. Phys. A **213**, 294 (1973).

[19] R. Dixon and R. Edge, Nucl. Phys. A **156**, 33 (1970).

[20] L. C. Lru, Chin. J. Phys. (Taiwan) **10**, 76 (1972).

[21] G. Din and J. Weil, Nucl. Phys. **86**, 509 (1966).

[22] P. Forsyth and R. Perry, Nucl. Phys. **67**, 517 (1965).

[23] J. Zhu, Y. Gao, L. Qin, Y. Sha, C. Jeynes, N. Peng, and Y. Wang, Nucl. Instrum. Methods Phys. Res., Sect. B **494-495**, 23 (2021).

[24] I. I. Bondouk and S. Saad, Atomkernenergie **29**, 270 (1977).

[25] C. E. Rolfs and W. S. Rodney, *Cauldrons in the Cosmos* (University of Chicago Press, Chicago, 1988)

[26] R. A. Malaney and W. A. Fowler, Astrophys. J. **345**, L5 (1989).